Available online at www.sciencedirect.com
ScienceDirect
Journal of the European Ceramic Society 30 (2010) 3125–3129
www.elsevier.com/locate/jeurceramsoc

Study on the effect and mechanism of zirconia on the sinterability of yttria transparent ceramic

Xiaorui Hou [a,b], Shengming Zhou [a,*], Wenjie Li [a,b], Yukun Li [a,b]

[a] *Key Laboratory of Materials for High Power Laser, Shanghai Institute of Optics and Fine Mechanics, Chinese Academy of Sciences, P.O. Box 800-211, Shanghai 201800, China*
[b] *Graduate School of Chinese Academy of Sciences, Beijing 100049, China*

Received 5 March 2010; received in revised form 9 June 2010; accepted 1 July 2010
Available online 1 August 2010

Abstract

Transparent Y_2O_3 ceramics were fabricated by solid-state reaction using high purity Y_2O_3 and ZrO_2 powder as starting material. The results indicated that ZrO_2 additive can improve the transparency of Y_2O_3 ceramic greatly. The best transmittance appears with 3 at.% ZrO_2 doped Y_2O_3 transparent ceramic with transmittance at 1100 nm of 83.1%, which is up to 98.6% of the theoretical value. The microstructure is uniform and no secondary phase is observed in the ceramic with the average grain size of 15 μm. The mechanism of ZrO_2 improving the transparency of Y_2O_3 ceramic is analyzed in detail. On this basis, Yb^{3+} doped Y_2O_3 transparent ceramic was also fabricated and spectroscopic properties were investigated.

Keywords: Y_2O_3; Transparent ceramics; Optical properties; Sintering

1. Introduction

Since the first laser demonstration on Nd:YAG polycrystalline ceramic in 1995,[1] more and more researches are focused on transparent ceramic laser materials.[2,3] Much progress has been made in improving the optical quality of ceramic as well as in exploring new laser materials.

Y_2O_3 is promising laser host material for trivalent lanthanide activators due to its superior properties such as refractory nature, stability, and optical clarity over a broad spectral range.[4] However, Y_2O_3 crystal is extremely difficult to fabricate because of high melting point (2430 °C) and phase transformation from cubic phase to high-temperature hexagonal phase at 2350 °C. Instead, transparent Y_2O_3 ceramic is easily prepared at low sintering temperature.

Conventionally, Y_2O_3 transparent ceramic has been fabricated by hot press or normal sintering with ThO_2, HfO_2 and La_2O_3 as additives.[5,6] However, these additives were not widely used for toxicity and high expense. In recent years, many methods have been studied to fabricate Y_2O_3 nanopowders which were finally sintered to transparent ceramic.[7,8] Unfortunately, most of these methods involve complicated steps and exposing in air for a long time, the transparency of ceramic is prone to decrease due to the pollution. Although Y_2O_3 transparent ceramic have been studied widely, ZrO_2 used as additive is less known to the best of our knowledge.[9] In this study, ZrO_2 was introduced as additive and Y_2O_3 transparent ceramics were sintered in vacuum. The effect of ZrO_2 on the sinterability of the ceramic was investigated systematically to obtain the optimum ZrO_2 doping concentration. On this basis, Yb^{3+} doped Y_2O_3 transparent ceramic was fabricated and the spectral properties were demonstrated.

2. Experimental

Y_2O_3 (99.999%, Changchun Ruipu Rare-Materials Co. Ltd., Changchun, China) and ZrO_2 (99.99%, Sinopharm Chemical Reagent Co. Ltd., Shanghai, China) with a manufacturer-determined particle size of 1 μm were used as starting materials. According to the formula of $(Y_{1.0-x}Zr_x)_2O_3$ (x = 0–0.10), the powders were blended and ball milled in absolute ethyl alco-

* Corresponding author. Tel.: +86 21 69918482; fax: +86 21 69918607.
E-mail addresses: xrhou1983@163.com (X. Hou), zhousm@siom.ac.cn (S. Zhou).

0955-2219/$ – see front matter © 2010 Elsevier Ltd. All rights reserved.
doi:10.1016/j.jeurceramsoc.2010.07.008

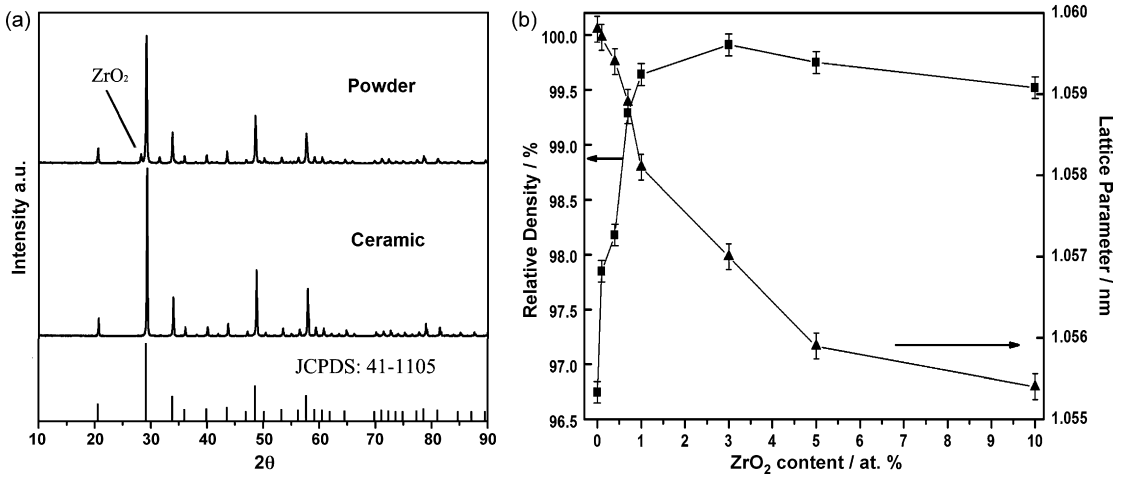

Fig. 1. (a) XRD patterns of 3 at.% ZrO_2 doped Y_2O_3 powder and sintered ceramic and (b) change of relative density and lattice parameter with ZrO_2 content.

hol for 24 h with agate balls. After dried at 130 °C overnight, the powder mixture was crushed and sieved through 200-mesh screen. Disks with 20 mm in diameter were compacted in steel mold at 15 MPa and then isostatically pressed at 250 MPa. Sintering was conducted at 1800 °C for 15 h in vacuum.

The structure of ceramic was determined by X-ray diffraction (XRD, Cu target, Model Ultima IV, Rigaku, Japan). The specimens (1.0 mm thick) were polished on both sides to measure optical transmittance with JASCO V-900 UV/VIS/NIR spectrophotometer. JSM 6360-LA scanning electron microscope (SEM) and energy-dispersive spectroscopy (EDS) were used to analyse the microstructure and component of the ceramics. Sintered density was measured by Archimedes' Principle. The fluorescence spectrum was acquired by a TRIAX 550 spectrophotometer with InGaAs LD as the pump source (excited at 940 nm).

3. Results

Fig. 1(a) shows XRD patterns of the powder and sintered ceramic. It was observed that except diffraction peaks of Y_2O_3, the diffraction peak corresponding to ZrO_2 was also detected in the milled powder. After sintered, the peak corresponding to ZrO_2 disappeared and the samples were well crystallized and coincided with cubic Y_2O_3 phase (Y_2O_3, JCPDS41-1105). The lattice parameter and relative density of these ceramics were calculated and shown in Fig. 1(b). The lattice parameter decreases with the increase of ZrO_2 content, which is mainly due to the smaller radius of Zr^{4+} ($R = 0.80$ Å) compared with Y^{3+} ($R = 0.90$ Å). The relative density increases rapidly with the content of ZrO_2, and the highest relative density is 99.91% for 3.0 at.% ZrO_2 doped transparent ceramic. It can be concluded that ZrO_2 can greatly increase the sintered density which is one of the definitive factors of transparency.

The photographs of Y_2O_3 ceramics with different concentration of ZrO_2 are provided in Fig. 2, which demonstrates that the addition of ZrO_2 improves the transmittance of Y_2O_3 ceramic to a great extent.

The microstructure of the polished surface was investigated after etched in H_3PO_4 for 3 min at 85 °C. As shown in Fig. 3(a), The microstructure of 3.0 at.% ZrO_2 doped Y_2O_3 ceramic was uniform and the grain size was comparatively homogeneous without abnormal grain growth. The grain size was measured by the grain size calculation software attached to the SEM and a mean linear intercept method, and the mean grain size was found to be 15 μm by averaging over 200 grains. The grain boundary is clear without pores or impurities. With ZrO_2 content increasing to 10.0 at.%, secondary phase was observed on the grain boundary as shown in Fig. 3(b). According to the EDS analysis, the mole ratio of Zr and Y elements is 13: 87 which is larger than the designed value of 10:90. It could be deduced that a fraction of ZrO_2 separated out from Y_2O_3–ZrO_2 solid solution and formed a secondary phase.

Fig. 4 presents the optical transmittance of Y_2O_3 transparent ceramics doped with different ZrO_2 content. With the increasing of ZrO_2 concentration, the transmittance increased and then gradually decreased. Using ZrO_2 as a dopant, the refractive index of ZrO_2 doped Y_2O_3 ceramic will slightly change and so is the theoretical transmission. We measured the refractive index of 3.0 at.% ZrO_2 doped Y_2O_3 ceramic as 1.82. The theoretical transmittance accurately calculated from the refractive index is

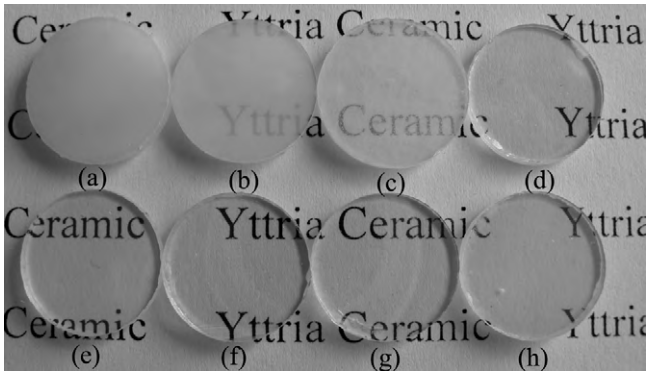

Fig. 2. Photographs of Y_2O_3 ceramics with different ZrO_2 content (a) 0, (b) 0.1 at.%, (c) 0.4 at.%, (d) 0.7 at.%, (e) 1.0 at.%, (f) 3.0 at.%, (g) 5.0 at.%, (h) 10.0 at.%.

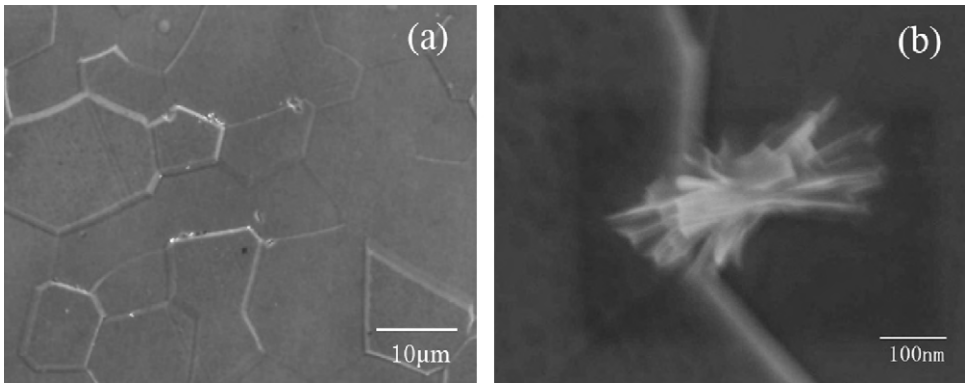

Fig. 3. Microstructure of Y_2O_3 transparent ceramics vacuum sintered at 1800 °C for 15 h (a) $(Y_{0.97}Zr_{0.03})_2O_3$ solid solution (b) Y_2O_3–10 at.%ZrO_2 two phase alloy.

84.3%.[10] The optimum result occurs with 3.0 at.% ZrO_2 and the transmittance at 1100 nm is 83.1%, which is up to 98.6% of the theoretical value. It can be seen from the phase diagram that the solid solution limit of ZrO_2 in Y_2O_3 is about 4.0 at.% at 1800 °C.[11] Alloy with 3.0 at.% ZrO_2 doped content was close to the solid solution limit and increase point defects to the extreme, which benefits for the elimination of pores and ceramic densification. However, increase in the ZrO_2 content beyond the solid solution limit, may lead to the precipitation of a secondary phase (Fig. 3(b)), which would cause the scattering of light in ceramic body and decrease the transparency.

After the optimum concentration of ZrO_2 (3.0 at.%) was obtained, 5.0 at.% Yb^{3+} doped Y_2O_3 transparent ceramic was obtained after sintering at 1800 °C for 15 h. The transmittance, absorption and emission spectra are given in Fig. 5. The samples demonstrates high transmittance not only in near infrared but also in visible region, as shown in Fig. 5(a), which indicates the sintered ceramics have high quality without scattering centers. From Fig. 5(b), we can see that the Yb:Y_2O_3 has a strong and broad absorption band around 950 nm, which matches well with the emission wavelength of InGaAs laser diodes. The absorption cross-section of Yb^{3+} can be calculated by Lambert' Law[12]:

$$\sigma_{abs} = \frac{\alpha}{C} \quad (1)$$

where α is the absorption coefficient, C is the concentration of Yb^{3+} ions. The absorption cross-sections at 947 nm and 973 nm are 0.959×10^{-20} and 1.175×10^{-20} cm^2, respectively, both of them are larger than that of Yb^{3+} doped yttrium lanthanum oxide transparent ceramic reported in Ref. [13]. Three emission peaks corresponding to the transition of $^2F_{5/2} \rightarrow {}^2F_{7/2}$ centered at 977 nm, 1032 nm and 1075 nm. Among them, the strongest peak is at 1032 nm with FWHM of 17 nm. The broad FWHM may play an active role in obtaining ultrashort pulse or femtosecond laser. Laser experiments will be reported in the near future.

4. Discussion

It was also reported that the transparent Y_2O_3 ceramic can be obtained without additive using Y_2O_3 nanopowder as raw material.[7] Nanopowder possesses narrow size distribution and high surface activity, which is beneficial for the sintering and transparency. As commercial powder was used in our experiment, due to the large size and poor dispersibility of the powder, transparency cannot be achieved without the addition of ZrO_2.

Combined with sintering kinetics, thermodynamics and experimental results above, the mechanism of ZrO_2 in improving the transparency of Y_2O_3 ceramic can be visualized as follows:

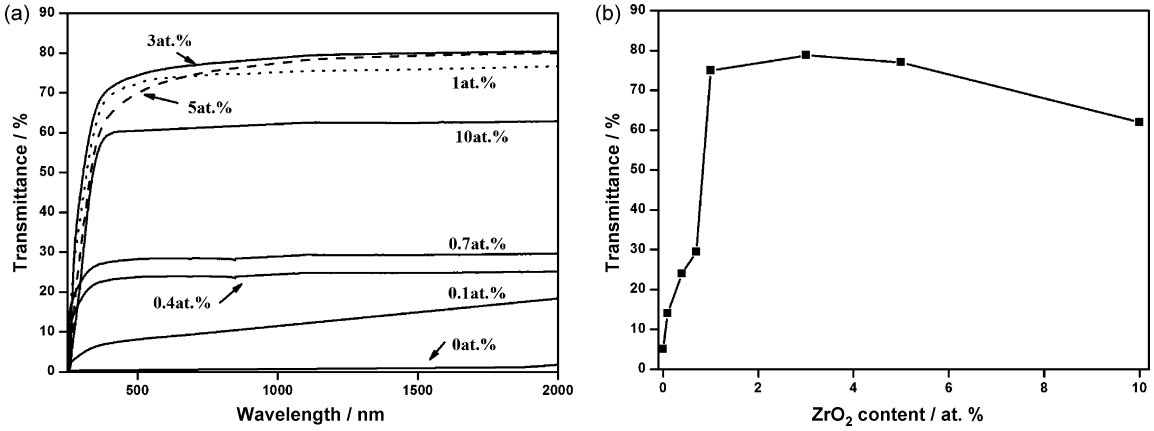

Fig. 4. Transmittance of Y_2O_3 transparent ceramics: (a) the transmittance spectra of Y_2O_3 transparent ceramics with different ZrO_2 content and (b) the change of transmittance at 1100 nm with the ZrO_2 content.

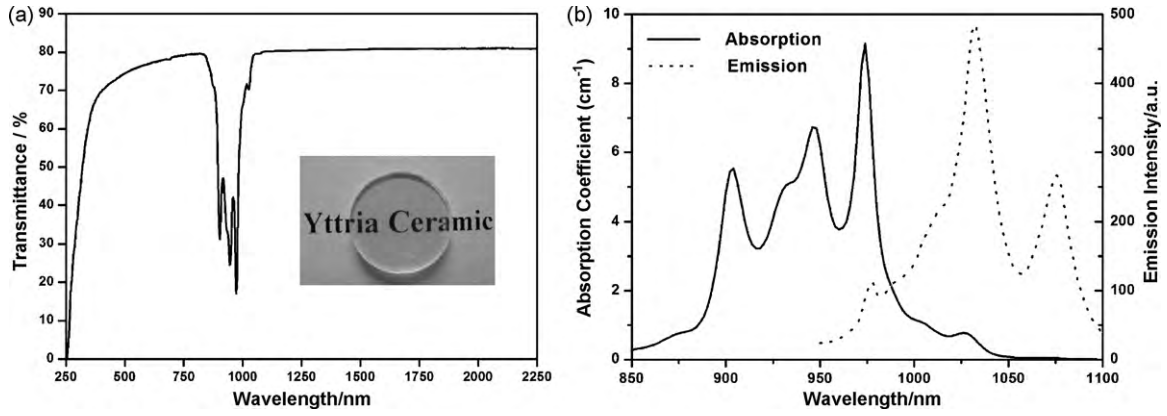

Fig. 5. (a) Transmittance spectra of $(Yb_{0.05}Y_{0.92}Zr_{0.03})_2O_3$ transparent ceramic and (b) absorption and emission spectra of $(Yb_{0.05}Y_{0.92}Zr_{0.03})_2O_3$ transparent ceramic.

(1) The addition of ZrO_2 decreases the melting point of ZrO_2–Y_2O_3 binary system,[11] and so is the sintering temperature.
(2) The radius of Zr^{4+} ($R = 0.80$ Å) is similar with that of Y^{3+} ($R = 0.90$ Å), which ensures small lattice distortion as Zr^{4+} substituting for Y^{3+}.
(3) In the final stage of sintering, a fraction of grains with low surface energy tend to grow to larger size on the consumption of surrounding smaller grains, which is known as discontinuous or exaggerated grain growth. During this process, owing to the high mobility of grain boundary, pores are easily embraced in the grains and cause the decrease of transparency. ZrO_2 is prone to form solid solution on the grain boundaries owing to its high melting point (2715 °C), which can hamper with the grain boundary mobility and occurrence of secondary recrystallization due to the solute drag mechanism. This benefits the elimination of pores and the uniformity of grain sizes, both of which are absolutely critical to transmittance.
(4) The sintering technology of transparent ceramic is different from that of ordinary ceramic which aims to increase sintering rate and shorten production period. However, for transparent ceramic, high sintering rate may result in closed porosity inside grains which is difficult to remove during sintering and cause the decreasing of the transparency. Indeed, it is known that the diffusion coefficient of oxygen anion is much higher than that of yttrium cation in pure Y_2O_3.[14] So cation diffusion is the rate-controlling step for grain boundary migration. Pei-Lin Chen also reported that the diffusion of $[Y_i^{\bullet\bullet\bullet}]$ dominates the grain boundary mobility.[15] We estimate the defect concentration in Y_2O_3 as follows:

Schottky defect:

$$Y_2O_3 \overset{\Delta G_S}{\longleftrightarrow} 2V_Y''' + 3V_O \tag{2}$$

Frenkel defect:

$$O_O \overset{\Delta G_F^A}{\longleftrightarrow} O''_i + V_O^{\bullet\bullet} \tag{3}$$

$$Y_Y \overset{\Delta G_F}{\longleftrightarrow} V_Y''' + Y_i^{\bullet\bullet\bullet} \tag{4}$$

The relationship between V_Y''', $Y_i^{\bullet\bullet\bullet}$ and O_i'' is deduced as:

$$[V_Y'''] = [O_i'']^{1.5} \left(\frac{K_S^{0.5}}{K_F^{A1.5}}\right) \exp\left[-\frac{\Delta G_S - 3\Delta G_F^A}{2kT}\right] \tag{5}$$

$$[Y_i^{\bullet\bullet\bullet}] = [O_i'']^{-1.5} \left(\frac{K_F K_F^{A1.5}}{K_S^{0.5}}\right) \exp\left[-\frac{2\Delta G_F - \Delta G_S + 3\Delta G_F^A}{2kT}\right] \tag{6}$$

In the above, K_S, K_F^A and K_F are the pre-exponential temperature-independent. ΔG_S, ΔG_F^A and ΔG_F are formation free energy of Schottky and Frenkel defect.

After ZrO_2 doping, the defect reaction is as follows:

$$2ZrO_2 \xrightarrow{Y_2O_3} 2Zr_Y^{\bullet} + O_i'' + 4O_O \tag{7}$$

It can be concluded by the above formula that every two Zr^{4+} create one O_i'', so that $[V_Y''']$ is increased but $[Y_i^{\bullet\bullet\bullet}]$ is decreased. The decreasing of $[Y_i^{\bullet\bullet\bullet}]$ concentration results in the slowdown of grain boundary mobility and sintering rate, which ensure the expelling of pores and densification of ceramic. The average grain size of ZrO_2 doped ceramic is 15 μm, which is much smaller than 50 μm reported in Ref. [2]. This also confirms that the addition of ZrO_2 decreases grain boundary mobility. Meantime, 3 at.% ZrO_2 doped sample lead the point defects to a appropriate mount. It is not only benefit for the expelling of pores, but also not too much to cause grey darkening which will bring decreasing of the transmittance in the visible range.[16]

5. Conclusion

Y_2O_3 transparent ceramics were fabricated by vacuum sintering technique with ZrO_2 as additive. 3 at.% ZrO_2 doped Y_2O_3 transparent ceramics had the best transmittance with the transmittance of 83.1% at 1100 nm. The microstructure is uniform and no secondary phase is observed in the ceramics with average grain size of 15 μm. The results showed that the introduction of ZrO_2 improves the transmittance of Y_2O_3 ceramic greatly and the mechanism of ZrO_2 improving the transparency of Y_2O_3

ceramic is analyzed in detail. With ZrO_2 as additive, 5.0 at.% Yb^{3+} doped Y_2O_3 transparent ceramic was also prepared. The absorption cross-sections at 947 nm ($\sigma_{abs} = 0.959 \times 10^{-20}$ cm^2) and 973 nm ($\sigma_{abs} = 1.175 \times 10^{-20}$ cm^2) are larger than that of Yb^{3+} doped yttrium lanthanum oxide transparent ceramic.

Acknowledgement

This work is supported by National Natural Science Foundation of China (No. 60676004).

References

1. Ikesue A, Kinoshita T, Kamata K, Yoshida K. Fabrication and optical properties of high-performance polycrystalline Nd:YAG ceramics for solid-state laser. *J Am Ceram Soc* 1995;**78**:1033–40.
2. Hao Q, Li W, Zeng H, Yang Q. Low-threshold and broadly tunable lasers of Yb^{3+}-doped yttrium lanthanum oxide ceramic. *Appl Phys Lett* 2008;**92**:211106.
3. Yagi H, Yanagitani T, Takaichi K. Characterizations and laser performances of highly transparent Nd^{3+}:$Y_3Al_5O_{12}$ laser ceramics. *Opt Mater* 2007;**29**:1258–62.
4. Takaichi K, Yagi H. Highly efficient Yb-doped Y_2O_3 ceramic lasers at 1030 nm and 1075 nm. *Appl Phys Lett* 2004;**84**:317–9.
5. Ikesue A, Kamata K, Yoshida K. Synthesis of transparent Nd-doped HfO_2–Y_2O_3 ceramics using HIP. *J Am Ceram Soc* 1996;**79**:359–64.
6. Dou C, Yang Q, Xu J. Luminescence behavior of Yb^{3+} heavy-doped yttrium lanthanum oxide transparent ceramics. *J Alloy Compd* 2009;**469**:282–5.
7. Wen L, Sun X. Synthesis of yttria nanopowders for transparent yttria ceramics. *Opt Mater* 2006;**29**:239–45.
8. Lemeshev DO, Lukin ES, Makarov NA. Prospects for creating new optically transparent materials with yttrium oxide and yttrium aluminum garnet. *Glass Ceram* 2008;**65**:25–7.
9. Bernard-Granger G. Sintering behavior and optical properties of yttria. *J Am Ceram Soc* 2007;**90**:2689–702.
10. J. Mouzon, Synthesis of Yb:Y_2O_3 nanoparticles and fabrication of transparent polycrystalline yttria ceramics. PhD thesis. Lulea University of Technology; 2005.
11. Duwez P, Brown FH. The zirconia–yttria system. *J Electrochem Soc* 1951;**98**:356–62.
12. Ingle JDJ, Crouch SR. *Spectrochemical analysis*. NJ: Prentice Hall; 1988.
13. Yang QH, Ding J, Zhang HW, Xu J. Investigation of the spectroscopic properties of Yb^{3+}-doped yttrium lanthanum oxide transparent ceramic. *Opt Commun* 2007;**273**:238–41.
14. Berard MF, Wilder DR. Cation self-diffusion in polycrystalline Y_2O_3 and Er_2O_3. *J Am Ceram Soc* 1969;**52**:85–8.
15. Chen Pei-Lin, Chen I-Wei. Grain boundary mobility in Y_2O_3: defect mechanism and dopant effect. *J Am Ceram Soc* 1996;**79**:1801–9.
16. Krell A, Klimke J, Hutzler T. Transparent compact ceramics: inherent physical issues. *Opt Mater* 2009;**31**:1144–50.